Author Manuscript

Author Manuscript

Author Manuscript

Author Manuscript

HHS Public Access

Author manuscript

J Orthop Res. Author manuscript; available in PMC 2019 March 01.

Published in final edited form as:

J Orthop Res. 2018 March ; 36(3): 979–986. doi:10.1002/jor.23716.

Optimizing a micro-computed tomography-based surrogate measurement of bone-implant contact

Matthew J. Meagher[1], **Rachna N. Parwani**[1,2,3], **Amarjit S. Virdi**[1], and **D. Rick Sumner**[1]

[1]Department of Cell & Molecular Medicine, Rush University Medical Center, Chicago, IL 60612

[2]Department of Bioengineering, University of Illinois at Chicago, Chicago, IL 60607

[3]College of Engineering, University of Portsmouth, Portsmouth, UK P01 3DJ

Abstract

Histology and backscatter scanning electron microscopy (bSEM) are the current gold standard methods for quantifying bone-implant contact (BIC), but are inherently destructive. Microcomputed tomography (μCT) is a non-destructive alternative, but attempts to validate μCT-based assessment of BIC in animal models have produced conflicting results. We previously showed in a rat model using a 1.5 mm diameter titanium implant that the extent of the metal-induced artefact precluded accurate measurement of bone sufficiently close to the interface to assess BIC. Recently introduced commercial laboratory μCT scanners have smaller voxels and improved imaging capabilities, possibly overcoming this limitation. The goals of the present study were to establish an approach for optimizing μCT imaging parameters and to validate μCT-based assessment of BIC. In an empirical parametric study using a 1.5 mm diameter titanium implant, we determined 90kVp, 88μA, 1.5μm isotropic voxel size, 1600 projections/180°, and 750 msec integration time to be optimal. Using specimens from an in vivo rat experiment, we found significant correlations between bSEM and μCT for BIC with the manufacturer's automated analysis routine ($r = 0.716$, $p = 0.003$) or a line-intercept method ($r = 0.797$, $p = 0.010$). Thus, this newer generation scanner's improved imaging capability reduced the extent of the metal-induced artefact zone enough to permit assessment of BIC.

Keywords

bone implant contact; microCT; metal artefact; osseointegration

Introduction

Successful integration of orthopaedic and dental implants with osseous tissue requires the formation of a direct interface between living bone and implant, a process known as osseointegration[1]. Osseointegration is measured via quantification of the amount of bone in direct contact with an implant, often called bone-implant contact (BIC). BIC is accepted to be an important predictor of the strength of implant fixation and has been extensively studied

Correspondence: D. Rick Sumner, Ph.D., Professor, Chair, Department of Cell & Molecular Medicine, Armour Academic Center, 600 S. Paulina St., Suite 507, Chicago, IL 60612, Phone: 312-942-5511, Fax: 312-942-5744, rick_sumner@rush.edu.

Author Manuscript Author Manuscript Author Manuscript Author Manuscript

via several techniques that are inherently destructive to the test sample, precluding subsequent additional analyses.

Light microscopy[1–3] and backscatter scanning electron microscopy (bSEM)[1; 4–6] are the current gold standards for quantifying BIC. However, these techniques require extensive sample processing, including resin or plastic embedding, sectioning, and surface preparation (grinding and polishing). Thus, these destructive techniques do not allow for direct correlations to be made between BIC and the important functional parameters of implant fixation strength. Additionally, artefacts introduced during the processing steps may not be easily discernable and neither technique allows for three-dimensional visualization of the bone-implant interface. Assessment of BIC by micro-computed tomography (μCT) presents a potential alternative approach which would allow for three-dimensional, *in situ* visualization of the bone-implant interface while preserving that interface for other assessments.

BIC measurements using μCT have been reported[7–20], but only a few studies have attempted to validate the technique[12; 13; 18; 20]. The validation reports have been conflicting where two studies found correlation between μCT-measured BIC and histology-measured BIC[12; 20], and the other two reported no correlation[13; 18].

We previously reported that a number of factors prevent accurate measurement of BIC with μCT, including the need to assess bone within 12 μm of the bone-implant interface, a metal-induced artefact zone which was greater than 12 μm, and scans with insufficiently small voxel sizes[13]. Recently introduced commercial laboratory μCT scanners have improved imaging capabilities, including smaller voxels and higher accelerating voltage. The goals of the present study were to establish a protocol for optimizing μCT imaging parameters to allow bone measurements to be made in proximity to metal implants and to validate μCT-based assessment of BIC in a rat model in which a 1.5 mm diameter titanium implant is placed in the intramedullary space.

Methods

Optimization of Scanning Parameters to Minimize Metal Artefact

In these in vitro tests, we used an implant of the same dimensions and composition as used in our in vivo rat experiments[21; 22]. A 1.5 mm diameter titanium (Ti) rod (Goodfellow, Coraopolis, PA) immersed in water was used to model an implant surrounded by tissue. The implant was scanned, perpendicular to its long axis, with μCT (Scanco 50, Scanco Medical, Wayne, PA). Voxel size, X-ray tube current, filtering, integration time, the number of projections/180° and the scaling of the brightness of reconstructed images (mu scaling) were varied (Table 1) to determine the parameters yielding the least amount of metal artefact. The beam hardening correction of 1200 mg HA/CCM was applied during reconstruction. For the evaluation of each parameter, the variable in question was changed while all other scanning parameters were kept constant. The effects of X-ray tube current (200 μA, 155 μA, 88 μA, and 44 μA) and filter (0.1 mm Cu and 0.5 mm Al) were tested using an isotropic voxel size of 2 μm. Then, the effect of voxel size (3.5 μm, 2.5 μm, 2 μm, and 1.5 μm) was evaluated. Finally, the effects of projections/180° (2000, 1500, and 1000), integration time (300 msec,

Author Manuscript Author Manuscript Author Manuscript Author Manuscript

750 msec, and 1200 msec), and mu scaling (2048 and 4096) were evaluated using 1.5 μm voxels.

The weighted average gray scale values were determined for consecutive concentric voxel rings around the implant. These averages decrease as a function of distance from the implant surface with high values representing zones where there are metal-induced artefacts. Imaging parameters were chosen to maximize the decrease in the weighted average grey scale values as a function of distance from the implant, targeting a greyscale value of 85 (875 HU), the minimum value for bone, on a standard 8-bit 0–255 scale.

The μCT scanner's automated program for estimating BIC evaluates bone volume per total volume (BV/TV) in four concentric rings of voxels and reports the value as the osseointegration volume per total volume (OV/TV), with the user assigning the location of the voxel rings to be evaluated (Fig. 1A). The optimal set of voxels for evaluation of $BIC_{\mu CT\text{-}OV/TV}$ was determined by selecting the set of four concentric voxel rings which were closest to the implant, but outside the artefact zone (i.e., where the target grey scale value first dropped below 85).

Correlation between BIC from μCT and bSEM

Specimens from previous studies in which Ti rods (1.5 mm diameter, 15 mm length, Goodfellow, Coraopolis, PA) had been implanted in a rat model for between 2 and 8 weeks were used[23; 24]. Specifically, we embedded the whole femur containing the implant in polymethylmethacrylate and then prepared a 1 mm thick slab from each sample by cutting perpendicular to the long axis of the bone and implant (Buehler Isomet 5000, Lake Bluff, IL). The slabs were assigned to either a training set or a validation set, each with 9 specimens.

BIC was calculated from the μCT data in two different ways: a line-intersect method ($BIC_{\mu CT\text{-}LI}$) and the manufacturer's osseointegration/total volume (OV/TV) method ($BIC_{\mu CT\text{-}OV/TV}$). Briefly, for $BIC_{\mu CT\text{-}LI}$, a test pattern with 48 evenly spaced lines radiating outward from the center of the implant through 360° was used and each intersection of test line with the surface of the implant was scored as positive or negative for bone (Fig. 1B)[13]. $BIC_{\mu CT\text{-}LI}$ is the ratio of intersections between the overlaid grid and the bone-implant interface which score positive for bone and the total number of intersections and reported as a value between 0.0 and 1.0. $BIC_{\mu CT\text{-}LI}$ was determined using 3 μCT slices which were separated by 12μm. $BIC_{\mu CT\text{-}OV/TV}$ was measured using a stack of 200 slices.

The $BIC_{\mu CT\text{-}OV/TV}$ method requires choosing thresholds for segmenting the implant and bone. The choice of threshold for segmenting the implant was determined by comparing the Ti area estimated by the program with the known area of the implant cross-section. The threshold of 180 was chosen to find the best match in bone architecture between the segmented (binary) and greyscale images (Supplementary Figure 1A), which corresponded to a local minima in the attenuation histogram (Supplementary Figure 1B).

The training set samples were imaged using 90kVp, 88μA, 1.5μm isotropic voxel size, 1600 projections/180°, based on the initial tests of the Ti rod in water. We tested three scan

Author Manuscript Author Manuscript Author Manuscript Author Manuscript

durations: 3 hour (integration time = 600, frame averaging = 3), 2 hour (integration time = 600, frame averaging = 2) and 1 hour (68 minutes, integration time = 750, frame averaging = 1). The optimum scan duration was defined using the training set by examining the strength of correlation of BIC as determined by μCT and bSEM. Then, the validation set samples were scanned and evaluated per these parameters and correlated with the corresponding BIC values obtained with bSEM.

The slabs were prepared for bSEM by grinding to approximately 0.5mm thickness (Phoenix 4000, Buehler, IL, USA) and polished using a soft trident polishing cloth (Buehler, IL, USA) with 3μm diamond suspension irrigation fluid (Metadi fluid, Buehler, IL, USA) and no carbon coating. The bSEM images (Hitachi S-3000N) were collected at 20kV, 10Pa, Variable Pressure. The bSEM image location corresponded to the middle μCT slice used in both μCT-based BIC determinations. BIC was assessed via the line-intersect method.

Statistical Analysis

SPSS (Version 19, Chicago, IL) software packages was used to analyze data. Pearson's coefficient (r) was calculated using SPSS. A $p \leq 0.05$ significance level was used for all statistical tests.

Results

Minimization of Metal-Induced Artefact

Tube voltage was held constant at the highest available option, 90 kVp, to maximize beam penetration through the sample. Scanning current, filter, voxel size, projections/180° and integration time were tested with the Ti rod scanned in water. The 88μA current reduced the magnitude of the metal-induced artefact compared to 155μA and 200μA (Fig 2A). While the 44 μA current appeared to reduce the artefact further, it was at the expense of beam flux. Thus, the 88μA was selected for the remaining scans. The 0.5mm Al filter minimized the width of the metal artefact zone compared to the 0.1 mm Cu filter (Fig. 2B). Using 88 μA and the 0.5 mm Al filter, we next tested for voxel size. The 1.5 μm voxel size minimized the width of the artefact zone compared to voxel sizes of 2, 2.5, and 3.5 μm. Use of 1.5 μm voxels resulted in a metal-induced artefact zone that extended outward 4.5 μm from the implant surface (Fig. 2C). For each voxel size tested, an artefact zone sufficient to impair bone measurement extended outward 3 voxels from the implant surface. Thus, the smallest voxel size tested yielded the narrowest artefact zone. No quantitative differences were observed by increasing the projections/180° from 1000 to 1500 to 2000 (Fig. 2D), integration time from 300 to 750 to 1200 ms (Fig. 2E), or reconstruction scaling between 2048 or 4096 (Fig. 2F) when using 88 μA, 0.5 mm Al filter and 1.5 μm voxels. Thus, the optimal scan settings were defined as 90 kVp voltage, 88 μA current, 1.5 μm voxel size, 0.5 mm Al filter, and 4096 (default) scaling. We recommend a minimum of 750 ms integration time to minimize the possibility of photon starvation.

Optimizing Scan Time in the Training Set

Using the optimal scanning parameters, we scanned the training set slabs with a combination of integration time and frame averaging that required approximately 1 (750 msec integration

Author Manuscript Author Manuscript Author Manuscript Author Manuscript

time, frame averaging = 1, 1600 projections/180°), 2 (600 msec integration time, frame averaging = 2, 1600 projections/180°), or 3 (600 msec integration time, frame averaging = 3, 1600 projections/180°) hours to complete. It was clear that the subjective quality of the 3 hour scans was better than the 1 hour scans (Fig. 3). Thus, we tested the effect of scan duration on the correlation between BIC as calculated with bSEM and μCT. The longer scan times did not improve the correlation (Table 2) so the 1 hour scan duration was selected for subsequent experiments.

While no quantitative difference was measured between scans with increasing projections/180° from 1000 to 1500 to 2000 (Fig. 2D), qualitatively images had fewer streaking artefacts as projections/180° increased. To maximize the quality of images for measurement of $BIC_{\mu CT\text{-}LI}$, we sought to balance the number of projections/180° with scan time. Scans with 1600 or fewer projections/180° did not increase scan time, while scans with more than 1600 projections/180° did increase the scan time. We chose 1600 projections/180° as optimal because it maximized the number of projections collected without increasing the scan time.

Validation Set

The samples in the validation set were scanned with the optimal parameters (90kVp, 88μA, 1.5μm isotropic voxel size, 1600 projections/180°, 750 msec integration time, 4096 scaling). A statistically significant correlation was observed between BIC_{bSEM} and $BIC_{\mu CT\text{-}OV/TV}$ ($r = 0.716$, $p = 0.003$, Fig. 4A) and $BIC_{\mu CT\text{-}LI}$ ($r = 0.797$, $p = 0.010$, Fig. 4B). $BIC_{\mu CT\text{-}OV/TV}$ was also correlated with $BIC_{\mu CT\text{-}LI}$ ($r = 0.785$, $p < 0.001$). $BIC_{\mu CT\text{-}LI}$ underestimates low BIC_{bSEM} values while overestimating high BIC_{bSEM} values (slope = 0.617, intercept = 0.161, Fig. 4A). In contrast, $BIC_{\mu CT\text{-}OV/TV}$ overestimates low BIC_{bSEM} values while underestimating high BIC_{bSEM} values (slope = 1.335, intercept = −0.314, Fig. 4B). Very thin rims of bone (less than 10μm thick) and very small gaps at the interface (less than 5μm in width) were visible in bSEM images, but these gaps were not resolved in the μCT images and the thin rims of bone were not easily defined (Fig. 5).

Discussion

In this study, we demonstrated the feasibility of using μCT to non-destructively evaluate BIC, preserving the bone-implant interface for other assays. While the μCT technology used in the present study enabled prediction of BIC, this technique required careful optimization of scan parameters. We used a systematic approach to optimizing μCT parameters and recommend that similar optimization be done if different scanners, implant materials, implant dimensions or bone sites are used.

Park *et al.* were the first group to attempt validation of μCT-generated images to measure BIC by quantitative comparison with a standard methodology, in their case histomorphometry. Their results showed that the two techniques were significantly linearly correlated although μCT underestimated BIC ($r = 0.855$)[12]. Park, *et al.* placed screw-shaped, commercially pure titanium implants with a length of 7 mm and an outer diameter of 3.75 mm trans-cortically in the tibia of New Zealand white rabbits[12]. μCT scanning was performed at a voxel size of 15.95 μm[12]. Park, *et al.* did not comment on the presence of a metal-induced artefact[12]. In contrast, Butz, *et al.* reported no significant correlation between

Author Manuscript Author Manuscript Author Manuscript Author Manuscript

peri-implant bone volume quantified via histology and bone volume quantified via μCT using a voxel size of 8 μm for a region of interest between 0 and 24 μm from the implant surface for unthreaded, titanium implants 1 mm in diameter and 2 mm in length placed into the femur of Sprague-Dawley rats[18]. They attributed the lack of correlation to a titanium-induced artefact, leading to an overestimated peri-implant bone volume compared to histology[18]. Similarly, we previously reported that the metal-induced artefact extended 48 μm away from the implant surface when using a voxel size of 16 μm and 24 μm away from the implant surface when using a voxel size of 8 μm[13]. We also reported that to obtain an accurate estimate of BIC, the bone volume needed to be measured accurately within 12 μm of the implant surface[13]. It is not clear why the results of Park *et al.*[12] differ from those of Butz *et al.*[18] and our previous study[13]. Possible factors accounting for the differences include differences in the μCT scanner used, thresholds chosen, the implant shape, and the implant placement location.

Stadelmann et al. found a strong correlation between BIC assessed via μCT and histology[20]. This strong correlation, in contrast to our own findings which showed a moderate correlation, is attributable to differences in the implant used. In Stadelmann, et al. a non-attenuating PEEK implant coated with a thin (30 μm) layer of titanium was implanted transcortically[20]. The thin titanium layer would be expected to have a much smaller metal-induced artefact than the 1.5 mm thick titanium implant we used.

The findings of the present study emphasize the importance of testing μCT imaging parameters. For most parameters, there is a trade-off between reducing the size of the metal-induced artefact and other considerations including scan time, field of view for a given voxel size, and size of implant. For instance, use of a low current results in a smaller X-ray focal spot size, thereby reducing source spot blurring and improving spatial resolution. However, too low of a current could result in insufficient radiation intensity and a depressed signal to noise ratio. Thus, while 44 μA was shown to minimize the metal induced artefact, we compromised between artefact minimization and maximization of signal-to-noise ratio by selecting 88μA. Similarly, while the 0.1 mm Cu filter could decrease beam hardening, the 0.5 mm Al filter improved image quality presumably because of increased radiation flux.

Changes to the number of projections and integration time did not yield improved correlations between bSEM and μCT, although they did result in qualitatively improved images. Theoretically, too few projections could result in missing data, leading to reconstruction artefacts, while insufficient integration time could lead to photon starvation resulting in a low signal-to-noise ratio. Despite these concerns, doubling or tripling the scan time did not result in an increased correlation between BIC measured with bSEM and μCT so we selected the most economical scan time.

By changing the mu scaling, the maximum brightness of an image can be increased or decreased. Briefly, the recorded linear attenuation value (mu value) is multiplied by a scaling factor (mu scaling) to produces an integer value. In our study, we began with the default mu scaling of 4096 and then reconstructed the images with a lower mu scaling of 2048 to minimize saturation in the image. Changing the mu scaling from the default of 4096 to 2048 did not improve the correlation between either $BIC_{\mu CT\text{-}LI}$ or $BIC_{\mu CT\text{-}OV/TV}$ and BIC_{bSEM}.

Author Manuscript Author Manuscript Author Manuscript Author Manuscript

Once the other imaging parameters were optimized, it became apparent that choice of voxel size had a major effect on determining how close to the bone-implant interface a measurement could be made. While the metal-induced artefact zone extended outward from the implant for 3 voxels in the present study regardless of voxel size, and in two other reports in the literature[13; 18], the voxel size determines the physical distance that the 3 voxel metal-induced artefact zone extends from the interface. We suspect that minimizing the voxel size may also be beneficial by reducing errors associated with partial volume effects.

Even with a voxel resolution of 1.5μm, very small gaps at the bone implant interface (less than 5μm) and very thin rims of bone (less than 10μm) could not be easily resolved via μCT in contrast to bSEM. This discrepancy in image quality between the two modalities presumably contributes to the less than perfect correlation between bSEM and μCT assessment of BIC. Additionally, these gaps would not be accounted for when evaluating $BIC_{\mu CT\text{-}OV/TV}$, as the voxels immediately adjacent to the bone-implant interface are excluded from analysis and this may account for the slightly better correlation when using $BIC_{\mu CT\text{-}LI}$ instead of $BIC_{\mu CT\text{-}OV/TV}$.

OV/TV, as evaluated by the μCT script, is a proxy measurement for BIC. BIC_{bSEM} and $BIC_{\mu CT\text{-}OV/TV}$ are not equivalent because they do not measure the same region. BIC_{bSEM} measures bone directly adjacent to the implant while $BIC_{\mu CT\text{-}OV/TV}$ measures the amount of bone in a region 4.5–10.5 μm from the bone-implant interface. Based on our previous empirical study[13], we propose that measurement of bone volume sufficiently close to the surface of the implant provides a surrogate approximation of the amount of bone in contact with the surface of the implant. Indeed, our finding of significant correlations between bSEM and μCT in the present study supports the validity of this previous finding.

We compared bSEM and μCT using two analysis strategies. In the first instance, we used a line-intersect method with each imaging modality. In the second instance, we used the line-intersect method with bSEM and a proxy measurement (OV/TV) with μCT. In comparing bSEM and μCT using the line-intersect method, the principal differences in imaging modalities include spatial resolution and the presence of a metal-induced artefact in μCT, both of which likely limited the strength of the correlation between bSEM and μCT using the line-intersect method. These imaging differences also likely explain why small interface gaps and very thin rims of bone which could be resolved with bSEM were not easily identified in the μCT images. In addition, it is likely that slight errors in registration of the bSEM and μCT images would also have been a limiting factor. The μCT-based OV/TV method assesses bone volume in a 4 voxel region of interest located 4.5 μm to 10.5 μm away from the implant surface that includes 200 slices (300 μm in the longitudinal direction). The rationale for making this proxy measurement was our previous demonstration that bone volume in this region is strongly correlated with BIC[13]. The present study shows that improvements in μCT instrumentation subsequent to our earlier report[13] have reduced the width of the metal-induced artefact zone enough to permit μCT-based OV/TV to serve as a proxy of BIC. However, neither μCT analysis strategy (the line-intersect method or the OV/TV method) provides perfect correlations with BIC.

Author Manuscript Author Manuscript Author Manuscript Author Manuscript

For other model systems (e.g., different species, implant geometry, or anatomic site), we recommend performing the type of optimization demonstrated here and in our previous report[13] to verify that the surrogate measurement provides a good estimation of BIC. In preliminary experiments, we have found that the distance the attenuation artefact extends beyond the implant edge is significantly impacted by the implant material, but not by implant diameter within the narrow range of diameters measured (Supplementary Figure 2).

This study demonstrates the feasibility of assessing BIC via non-destructive μCT using either manual or automated assessment of the μCT images. An advantage of the automated method includes more extensive sampling of the interface, but at the cost of somewhat reduced ability to estimate BIC. We believe that the small degradation in correlation when using the automated method is justified.

Overall μCT offers several advantages over labor intensive and destructive techniques such as histology and bSEM to measure BIC, including the ability to assess implant fixation or other end points in the same samples. A limitation of using μCT is that while both $BIC_{\mu CT\text{-}LI}$ and $BIC_{\mu CT\text{-}OV/TV}$ are correlated with BIC_{bSEM}, the correlation values are moderate ($r \sim 0.7–0.8$). In comparison studies, this level of correlation is probably sufficient, but if the true BIC value is needed, it would be necessary to use the regression equations to estimate the true BIC or to use gold standard methods. If additional endpoints are being reported, such as mechanical testing, then $BIC_{\mu CT\text{-}OV/TV}$ may be sufficient since it provides correlated information while preserving the bone-implant interface for other types of analysis.

Future studies to identify image or signal processing techniques to filter noise and extract more information from the μCT images should serve to further minimize metal-induced artefacts and may improve the ability to measure BIC non-destructively.

Importantly, this study establishes a systematic method for the optimization and validation of the measurement of BIC via μCT. This method could be employed to facilitate the use of μCT to measure BIC with other model systems and implant geometries and to enable additional comparisons between μCT-based measurements and evaluations via other techniques such as histology.

Conclusions

This study demonstrates that with optimization of scanning parameters, metal-induced artefacts can be minimized sufficiently to enable quantification of BIC via μCT.

Supplementary Material

Refer to Web version on PubMed Central for supplementary material.

Acknowledgments

Research reported in this paper was supported by National Institute of Arthritis and Musculoskeletal and Skin Diseases of the National Institutes of Health under award number R01AR066562. The content is solely the responsibility of the authors and does not necessarily represent the official views of the National Institutes of Health. Support from the Grainger Foundation was also used. MicroCT scanning was performed at the Rush University Medical Center MicroCT/Histology Core.

Author Manuscript Author Manuscript Author Manuscript Author Manuscript

Funding Source: NIH R01 AR066562 and the Grainger Foundation

References

1. Albrektsson T, Branemark PI, Hansson HA, et al. Osseointegrated titanium implants. Requirements for ensuring a long-lasting, direct bone-to-implant anchorage in man. Acta Orthopaedica Scandinavica. 1981; 52:155–170. [PubMed: 7246093]
2. Branemark R, Branemark PI, Rydevik B, et al. Osseointegration in skeletal reconstruction and rehabilitation: a review. Journal of Rehabilitation Research and Development. 2001; 38:175–181. [PubMed: 11392650]
3. Stadlinger B, Pilling E, Huhle M, et al. Influence of extracellular matrix coatings on implant stability and osseointegration: An animal study. J Biomed Mater Res B Appl Biomater. 2007; 83:222–231. [PubMed: 17318830]
4. Lin H, Xu H, Zhang X, et al. Tensile tests of interface between bone and plasma-sprayed HA coating-titanium implant. J Biomed Mater Res. 1998; 43:113–122. [PubMed: 9619429]
5. Sovak G, Weiss A, Gotman I. Osseointegration of Ti6Al4V alloy implants coated with titanium nitride by a new method. Journal of Bone and Joint Surgery. 2000; 82:290–296.
6. Svehla M, Morberg P, Zicat B, et al. Morphometric and mechanical evaluation of titanium implant integration: comparison of five surface structures. Journal of Biomedical Materials Research. 2000; 51:15–22. [PubMed: 10813740]
7. Seitz P, Ruegsegger P. Anchorage of femoral implants visualized by modified computed tomography. Arch Orthop Trauma Surg. 1982; 100:261–266. [PubMed: 7159198]
8. Sakae T, Hayakawa T, Kimishiko H, et al. Potential Application of Micro-CT for Study of Bone-Ti Implant Interface. Journal of Hard Tissue Biology. 2000; 9:15–17.
9. Van Oosterwyck H, Duyck J, Vander Sloten J, et al. The Use of Microfocus Computed Tomography as a New Technique for Characterizing Bone Tissue Around Oral Implants. Journal of Oral Implantology. 2000; 26:5–12. [PubMed: 11831302]
10. Kiba H, Hayakawa T, Oba S, et al. Potential application of high-resolution microfocus X-ray techniques for observation of bone structure and bone-implant interface. Int J Oral Maxillofac Implants. 2003; 18:279–285. [PubMed: 12705308]
11. Sennerby L, Wennerberg A, Pasop F. A new microtomographic technique for non-invasive evaluation of the bone structure around implants. Clin Oral Implants Res. 2001; 12:91–94. [PubMed: 11168276]
12. Park YS, Yi KY, Lee IS, et al. Correlation between microtomography and histomorphometry for assessment of implant osseointegration. Clin Oral Implants Res. 2005; 16:156–160. [PubMed: 15777324]
13. Liu S, Broucek J, Virdi AS, et al. Limitations of using micro-computed tomography to predict bone-implant contact and mechanical fixation. J Microsc. 2012; 245:34–42. [PubMed: 21919905]
14. Stoppie N, van der Waerden J-P, Jansen JA, et al. Validation of Microfocus Computed Tomography in the Evaluation of Bone Implant Specimens. Clinical Implant Dentistry and Related Research. 2005; 7:87–94. [PubMed: 15996355]
15. Rebaudi A, Koller B, Laib A, et al. Microcomputed Tomographic Analysis of the Peri-Implant Bone. The International Journal of Periodontics & Restorative Dentistry. 2004; 24:3–11.
16. Xing Z, Hasty KA, Smith RA. Administration of pamidronate alters bone-titanium attachment in the presence of endotoxin-coated polyethylene particles. J BiomedMater ResB ApplBiomater. 2006; 83:354–358.
17. Gabet Y, Kohavi D, Voide R, et al. Endosseous implant anchorage is critically dependent on mechanostructural determinants of peri-implant bone trabeculae. J Bone Miner Res. 2010; 25:575–583. [PubMed: 19653813]
18. Butz F, Ogawa T, Chang TL, et al. Three-dimensional bone-implant integration profiling using micro-computed tomography. Int J Oral Maxillofac Implants. 2006; 21:687–695. [PubMed: 17066629]

Author Manuscript Author Manuscript Author Manuscript Author Manuscript

19. Vandeweghe S, Coelho PG, Vanhove C, et al. Utilizing micro-computed tomography to evaluate bone structure surrounding dental implants: a comparison with histomorphometry. J Biomed Mater Res B Appl Biomater. 2013; 101:1259–1266. [PubMed: 23661363]

20. Stadelmann VA, Potapova I, Camenisch K, et al. In Vivo Micro CT monitoring of osteomyelitis in a rat model. Bio Med research international. 2015

21. Liu S, Virdi AS, Sena K, et al. Bone turnover markers correlate with implant fixation in a rat model using LPS doped particles to induce implant loosening. Journal of Biomedical Materials Research Part A. 2012; 100A:918–928.

22. Liu S, Virdi AS, Sena K, et al. Sclerostin antibody prevents particle-induced implant loosening by stimulating bone formation and inhibiting bone resorption in a rat model. Arthritis & Rheumatism. 2012; 64:4012–4020. [PubMed: 23192793]

23. Irish J, Virdi AS, Sena K, et al. Implant placement increases bone remodeling transiently in a rat model. J Orthop Res. 2013; 31:800–806. [PubMed: 23280449]

24. Virdi AS, Irish J, Sena K, et al. Sclerostin antibody treatment improves implant fixation in a model of severe osteoporosis. J Bone Joint Surg Am. 2015; 97:133–140. [PubMed: 25609440]

Author Manuscript Author Manuscript Author Manuscript Author Manuscript

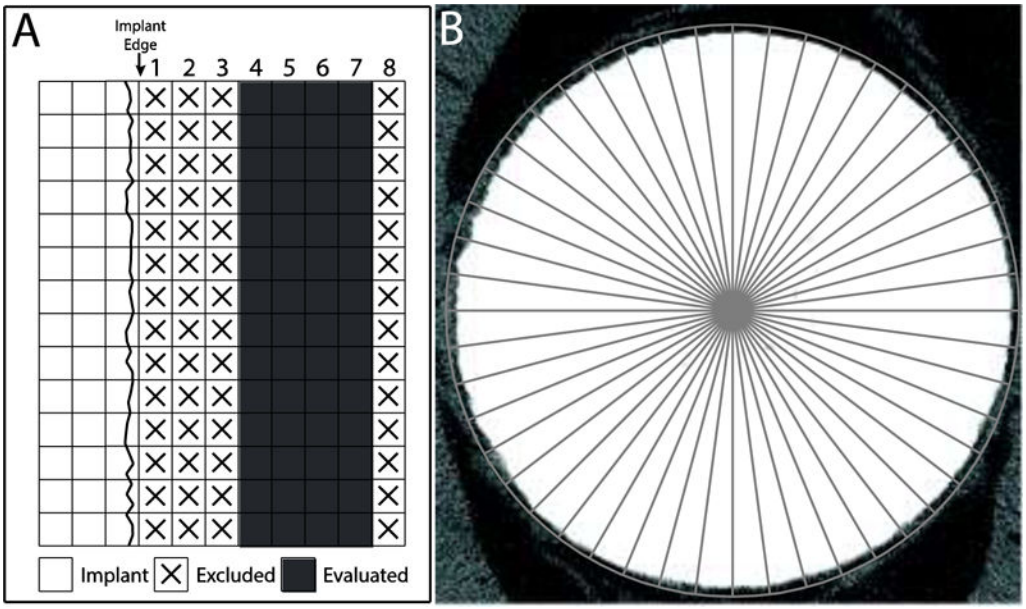

Figure 1.

(A) This schematic of a μCT image of a Ti implant depicts voxels overlaid on a cartoon of the implant. Voxel ring numbering begins adjacent to the implant edge. We used the manufacturer-provided script to evaluate bone-implant contact ($BIC_{\mu CT\text{-}OV/TV}$), which assesses bone volume per total volume (BV/TV) in voxels 4–7, ignoring the first 3 voxels adjacent to the implant interface. (B) BIC_{bSEM} and $BIC_{\mu CT\text{-}LI}$ were assessed via a line-intersect method. A circular test grid with 48 evenly distributed test lines radiating from the implant center was used with each intersection of the test line and implant surface being scored as positive or negative for bone (titanium implant is 1.5 μm in diameter).

Author Manuscript Author Manuscript Author Manuscript Author Manuscript

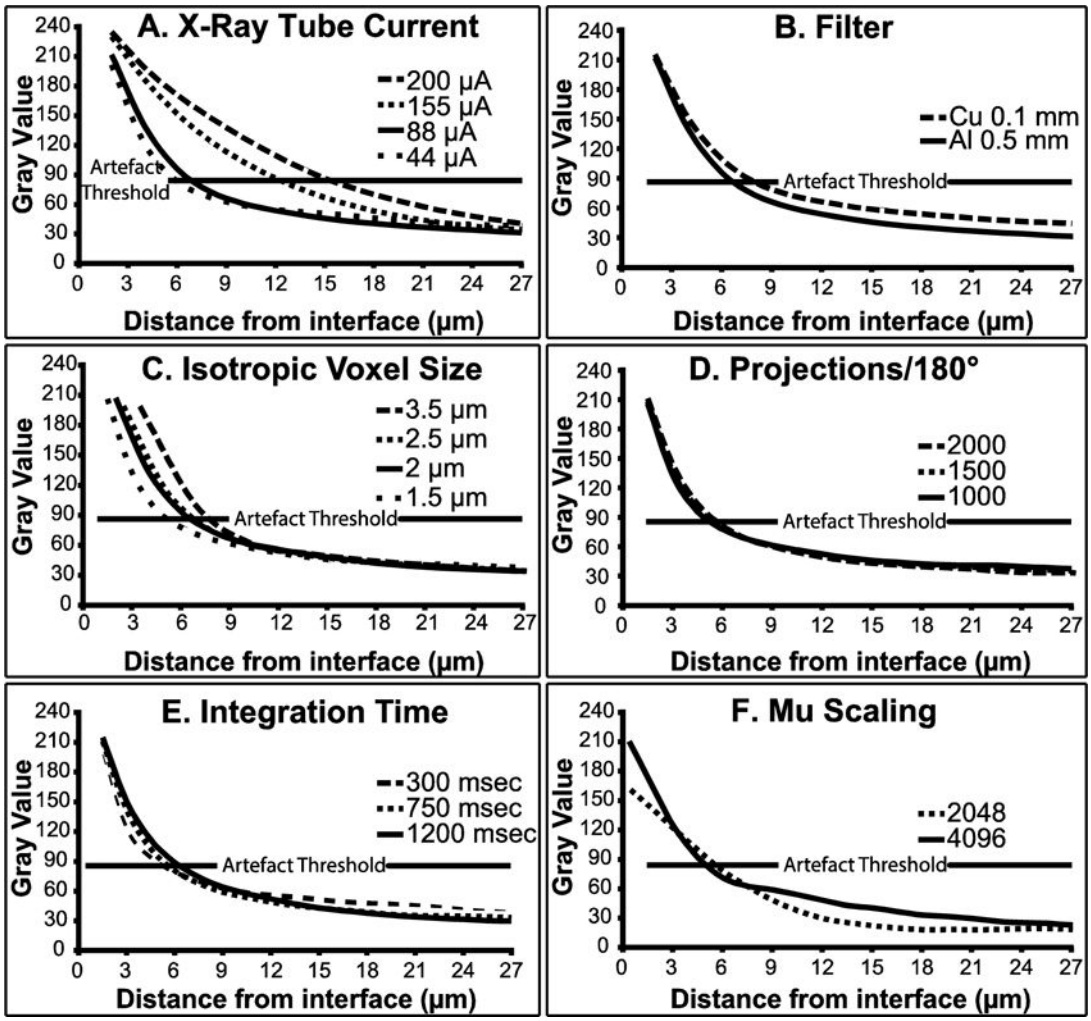

Figure 2.

The graphs plot the weighted average gray scale value as a function of distance from the implant interface for a 1.5 mm Ti diameter implant scanned in water. We chose 85 as the acceptable artefact threshold. Variables examined include (A) current (90kVp, 2 µm isotropic voxel size, 1600 projections/180°, 0.5 mm Al filter, 4096 mu scaling, and 800 msec integration time), (B) beam filtration (90kVp, 88 µA, 2 µm isotropic voxel size, 1600 projections/180°, 4096 mu scaling, and 800 msec integration), (C) voxel size (90kVp, 88 µA, 1600 projections/180°, 0.5mm Al filter, 4096 mu scaling, and 800 msec integration), (D) projections/180° (90kVp, 88 µA, 1.5 µm isotropic voxel size, 0.5 mm Al filter, 4096 mu scaling, and 800 msec integration), (E) and integration time (90kVp, 88 µA, 1.5 µm isotropic voxel size, 1600 projections/180°, 0.5 mm Al filter, and 4096 mu scaling), and (F) mu scaling (90kVp, 88 µA, 1.5 µm isotropic voxel size, 1600 projections/180°, 0.5 mm Al filter, and 750 msec integration).

Author Manuscript Author Manuscript Author Manuscript Author Manuscript

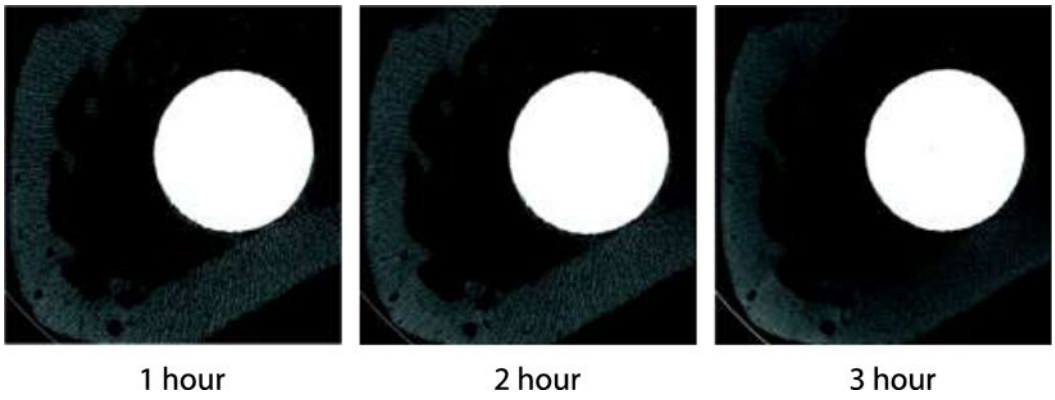

Figure 3.

The same specimen was scanned at the optimal imaging parameters (90kVp, 88μA, 1.5μm isotropic voxel size, 1600 projections/180°, and 750 msec integration time), varying the scan time from 1 hour to 3 hours. Lengthening scan times produces qualitatively better images. The implant is 1.5 mm in diameter.

Author Manuscript Author Manuscript Author Manuscript Author Manuscript

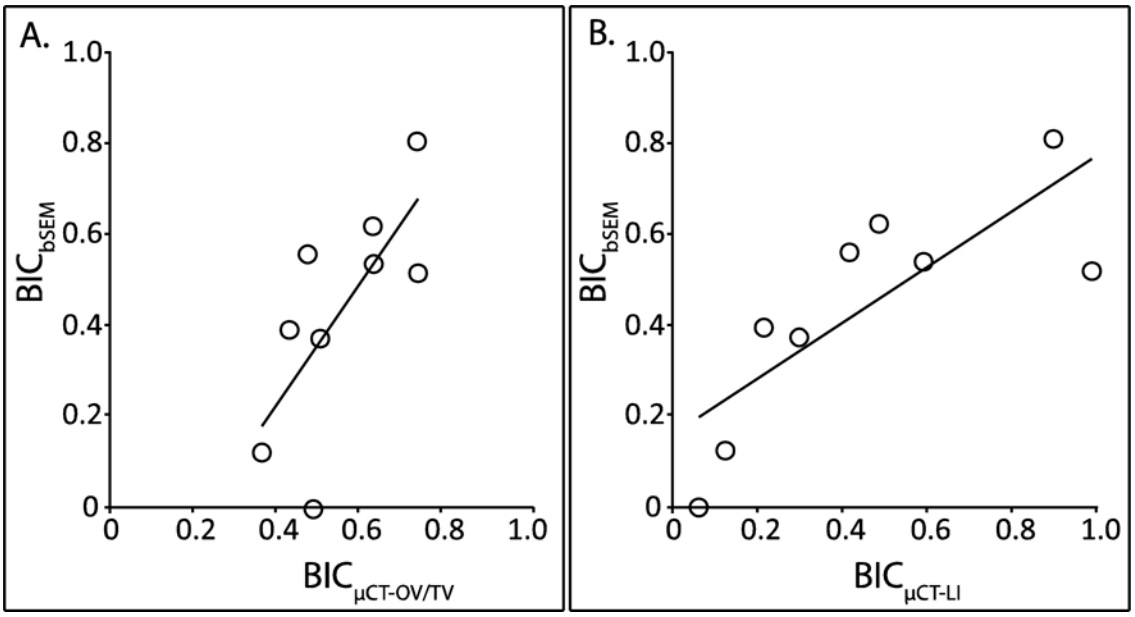

Figure 4.

(A) In the validation set, $BIC_{\mu CT\text{-}OV/TV}$ was significantly correlated with BIC_{bSEM} (r = 0.716, $p = 0.003$, $BIC_{bSEM} = 1.335*BIC_{\mu CT\text{-}OV/TV}-0.314$). (B) In the validation set, $BIC_{\mu CT\text{-}LI}$ was significantly correlated with BIC_{bSEM} (r = 0.797, $p = 0.010$, $BIC_{bSEM} =0.617*BIC_{\mu CT\text{-}LI} +0.161$).

Author Manuscript Author Manuscript Author Manuscript Author Manuscript

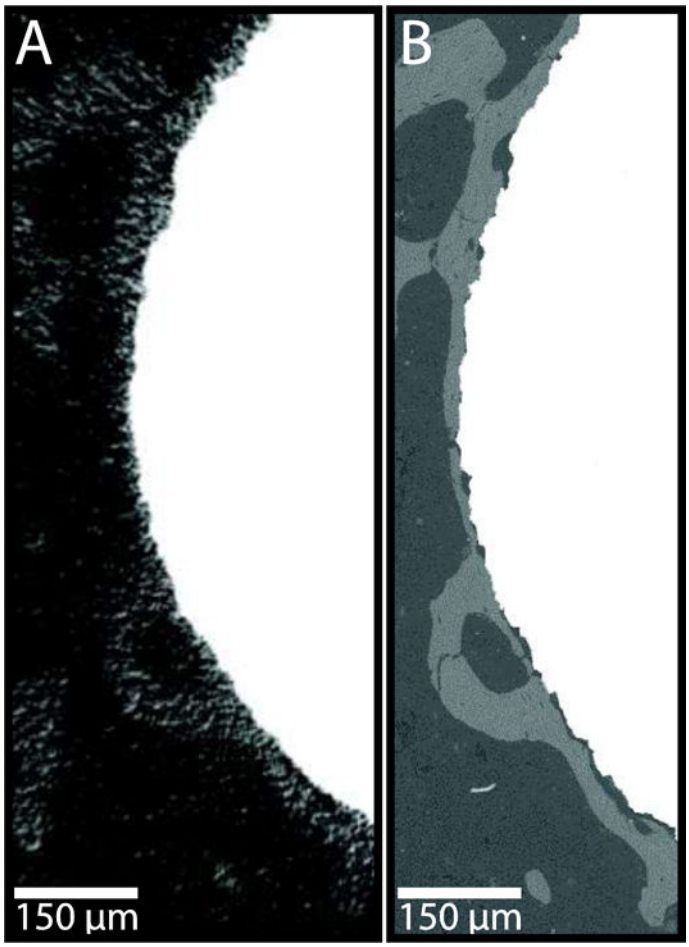

Figure 5.
Representative images of peri-implant bone as visualized by (A) µCT and (B) bSEM. Note the enhanced resolution of bone features close to the implant surface in (B) compared to (A). Image is enlarged 60×.

Author Manuscript Author Manuscript Author Manuscript Author Manuscript

Table 1

A summary of the values tested for each μCT scanning parameter varied to identify the optimal scan settings for the minimization of metal artefacts.

Scanning Parameter	Values Tested				Model used to test
Voxel Size (μm)	3.5	2.5	2	1.5	Ti pin in water
X-ray Tube Current (μA)	200	155	88	44	Ti pin in water
Integration Time (ms)	300	750	1200		Ti pin in water
# Projections/180°	1000	1500	2000		Ti pin in water
Filtering (mm)	0.5 Al	0.1 Cu			Ti pin in water
Mu scaling	4096	2048			Ti pin in water
Frame averaging	3	2	1		Training set

J Orthop Res. Author manuscript; available in PMC 2019 March 01.

Author Manuscript

Author Manuscript

Author Manuscript

Author Manuscript

Table 2

Correlation between BIC_{bSEM} and $BIC_{\mu CT\text{-}LI}$ for 1, 2, and 3 hour scan durations in the training set. Longer scan time did not increase the correlation between BIC_{bSEM} and $BIC_{\mu CT\text{-}LI}$.

Training Set Correlation BIC_{bSEM} and $BIC_{\mu CT\text{-}LI}$			
Time (hour)	**1**	**2**	**3**
Pearson's Coefficient (r)	0.839	0.878	0.854
p	0.037	0.021	0.030